Oblong-Shaped VCSELs with Pre-Defined Mode Patterns

A. Gadallah and A. Kroner

We report fabrication and characterization of a novel type of vertical-cavity surface-emitting laser (VCSEL). A dotted surface etch in an oblong-shaped output aperture is utilized to select a certain higher-order transverse mode. Optical trapping and particle manipulation are attractive applications for these VCSELs.

1. Introduction

VCSELs, which emit from the planar surface of the wafer rather than from the cleaved end facets, have been extensively investigated over the last years. The main advantages of these devices over the conventional edge-emitting lasers lie in their spatial and spectral output properties as well as manufacturing, testing, and packaging at lower cost. Because of their suitability for monolithic integration into two-dimensional arrays, VCSELs pave the way for a large variety of applications, such as space-parallel optical communication technologies or optical sensing and lighting using high-power sources. A new and attractive application of VCSELs in biophotonics is optical trapping, where active manipulation of biological cells [1], stacking and translation of microscopic particles [2], as well as a miniaturized system, the so-called integrated optical trap [3], were already successfully demonstrated. In order to sort particles using such an integrated optical trap, we intend to selectively deflect them from their initial flow direction with the trapping forces of a tilted, continuously emitting VCSEL array as described in [4] and the preceding article in this Annual Report. In order to create the required closely spaced intensity maxima, here we introduce a novel VCSEL which oscillates on a pre-defined high-order mode.

2. Fabrication and Simulation

A photograph of the new oblong-shaped VCSEL is shown in Fig. 1. The dotted surface etch is utilized to stimulate a certain transverse mode. There are two main differences between this specially designed VCSEL and a standard device. Firstly, concerning the layer structure, a quarter-wavelength anti-phase layer is added in order to induce a decrease in top mirror reflectivity. This layer is then selectively removed by means of wet-chemical etching. The second point concerns the shape of the mesa and thus of the oxide aperture. It is no longer of circular shape, instead it is rectangular, where one side of the rectangle is much longer than the other. The layer structure consists of 23 C-doped

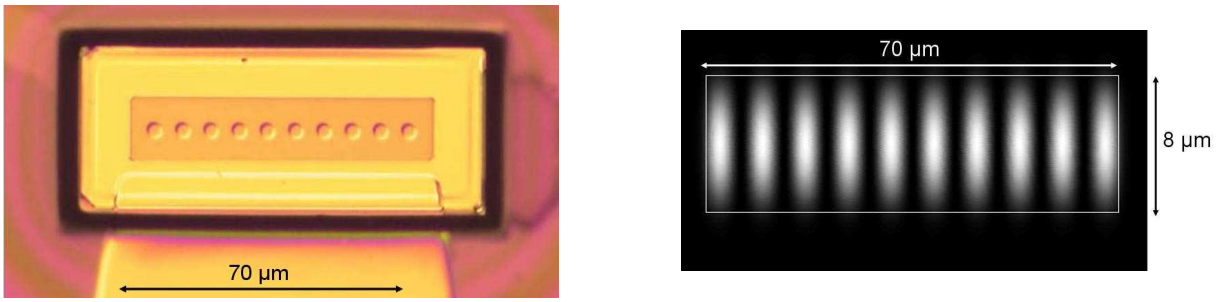

Fig. 1: Photograph of an oblong-shaped VCSEL with a $70 \times 8\,\mu m^2$ size oxide aperture and a 10-spot surface relief pattern (left). Simulated intensity profile of the selected high-order mode (right).

GaAs/AlGaAs p-distributed Bragg reflector (DBR) pairs as top mirror (plus the topmost GaAs quarter-wave layer), 38.5 Si-doped n-DBR pairs as the bottom mirror, and three 8 nm thick GaAs quantum wells for laser emission around 850 nm wavelength. Current confinement is achieved through thermal oxidation of an AlAs layer placed just above the one-wavelength thick inner cavity. Wet etching is used to reach this layer. N- and p- type metallization processes are applied, followed by polyimide passivation. Finally, bond-pad metallization is carried out for electrical contacting. Concerning the simulation of the transverse modes supported by the VCSEL cavity, the following approach is taken: We assume a rectangular semiconductor core of refractive index n_1, which corresponds to the non-oxidized cross-sectional area of the cavity, surrounded by a cladding layer of refractive index $n_2 < n_1$. The indices n_1 and n_2 are interpreted as average numbers in the longitudinal cavity direction. The index difference $\Delta n = n_1 - n_2$ is related to the cavity resonance shift $\Delta\lambda_{ox}$ as [5]

$$\Delta n = n_1 \Delta\lambda_{ox}/\lambda \ , \tag{1}$$

where λ is the lasing wavelength. The parameter $\Delta\lambda_{ox}$ is easily determined from two calculations with the transfer matrix method [5] as the difference in resonance wavelengths in the non-oxidized and oxidized parts of the cavity. With known indices n_1 and n_2, we then solve the Helmholtz equation in the transverse plane while applying the Dirichlet boundary conditions, i.e., the electric field diminishes at the boundary of the calculation window. The result is a usually large number of guided transverse modes. The simulated intensity profile for one such mode for oxide aperture dimensions of 8 µm width and 70 µm length is illustrated in Fig. 1 (right), where the calculation window is $18\,\mu m \times 80\,\mu m$. Its two dimensional mode order can be denoted as $(1, 10)$. In order to select this mode as the main lasing mode of the VCSEL, the anti-phase layer is selectively removed at positions coinciding with the calculated intensity maxima. The resulting surface relief is well visible in Fig. 1 (left).

3. Experimental Results

The light–current–voltage (LIV) characteristics of several oblong-shaped VCSELs without surface modification are displayed Fig. 2 (left), where dimensions (width × length) of the devices, e.g. $4\,\mu m \times 30\,\mu m$, are indicated. With increasing width, both the laser

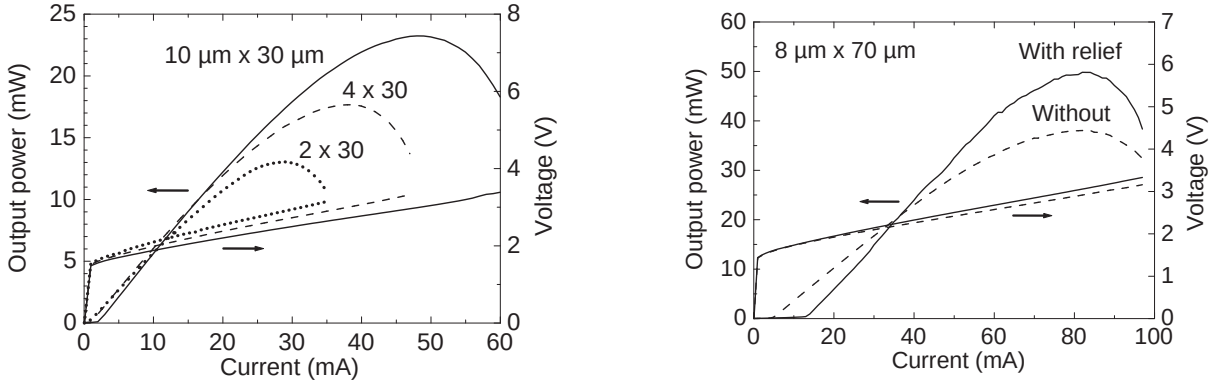

Fig. 2: LIV characteristics of standard oblong-shaped VCSELs of different size (left) and of a relief device in comparison with its reference (right).

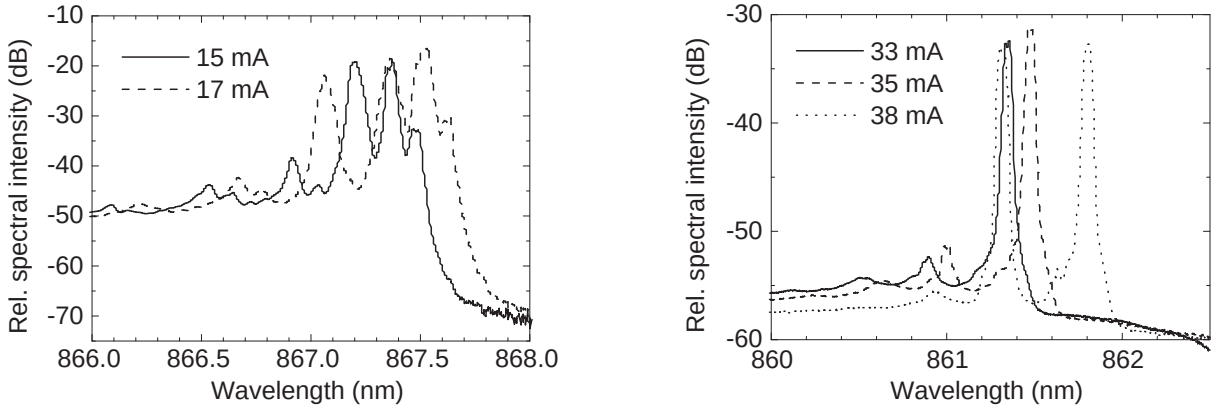

Fig. 3: Laser emission spectra of the standard $(8 \times 70)\,\mu m^2$ VCSEL (left) and of the corresponding relief device (right) according to Fig. 2 (right), both at different laser currents.

threshold current and the output power increase. For instance the laser threshold current and maximum output power are 0.9 mA and 17.5 mW, respectively, at 4 µm width. These values increase to 2 mA and 23.3 mW when the width of the device is 10 µm. On the other hand, it is worth to mention that the threshold current density increases with decreasing width, which is attributed to an increase of diffraction and scattering losses.

A comparison between the LIV characteristics of a reference oblong-shaped VCSEL and a relief device is made in Fig. 2 (right). Both the threshold current and the maximum output power of the relief device are increased, the latter to as much as 50 mW. This is caused by the reduction of the effective top mirror reflectivity. The laser spectra emitted from a standard $(8 \times 70)\,\mu m^2$ VCSEL are shown in Fig. 3 (left) for two different currents. Multiple transverse modes oscillate simultaneously even near threshold. On the other hand, there is a tendency for suppression of these higher-order modes in case of the relief devices, as shown in Fig. 3 (right). In order to identify the main mode in the spectrum in Fig. 3 (right), we have performed a spectrally resolved near-field measurement by scanning a lensed fiber tip over the output aperture with high resolution. Figure 4 shows the near-field intensity pattern of the VCSEL from Fig. 1 (left), having 10 etch spots, each 4 µm wide. The data are recorded at 31 mA current (see Fig. 2, right). The measured and

simulated (Fig. 1, right) spectra are similar, however, the former exhibits 9 instead of 10 maxima as well as some irregularities. Currently we attribute these effects to the gradient in layer thickness incorporated during molecular beam epitaxial growth, which induces a cavity resonance shift along the device length.

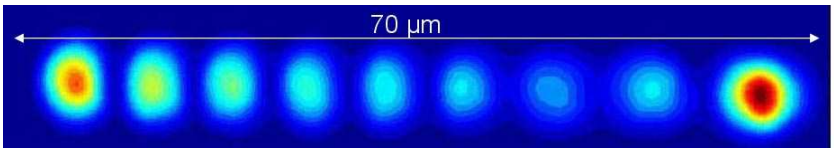

Fig. 4: Near-field intensity pattern of the oblong-shaped VCSEL from Fig. 1 (left), recorded at 31 mA current (see Fig. 2, right). The wavelength is 865 nm.

4. Conclusions

Design, fabrication, and characterization of oblong-shaped VCSELs with large length-to-width ratio of the oxide aperture have been carried out. For very narrow widths, scattering and diffraction losses increase the threshold current density. A dotted surface etch is employed to select a defined mode with order $(1, N)$, where N is a large integer. The surface relief reduces the mirror reflectivity and increases both the threshold current as well as the peak output power. First mode-controlled devices have been realized, however, the selection mechanism needs further improvement.

References

[1] A.L. Birkbeck, R.A. Flynn, M. Ozkan, D. Song, M. Gross, and S.C. Esener, "VCSEL arrays as micromanipulators in chip-based biosystems", in *Biomedical Microdevices*, vol. 5, no. 1, pp. 47–54, 2003.

[2] F. Sumiyama, Y. Ogura, and J. Tanida, "Stacking and translation of microscopic particles by means of 2 × 2 beams emitted from a vertical-cavity surface-emitting laser array", *Appl. Phys. Lett.*, vol. 82, no. 18, pp. 2969–2971, 2003.

[3] A. Kroner, I. Kardosh, F. Rinaldi, and R. Michalzik, "Towards VCSEL-based integrated optical traps for biomedical applications", *Electron. Lett.*, vol. 42, no. 2, pp. 93–94, 2006.

[4] A. Kroner, A. Gadallah, I. Kardosh, F. Rinaldi, and R. Michalzik, "Integrated VCSEL trap arrays for microfluidic particle separation and sorting", in Proc. *EOS Topical Meeting on Biophotonics and Biomedical Optics*, pp. 140–141. Paris, France, Oct. 2006.

[5] R. Michalzik and K.J. Ebeling, "Operating Principles of VCSELs", Chap. 3 in *Vertical-Cavity Surface-Emitting Laser Devices*, H. Li and K. Iga (Eds.), pp. 53–98. Berlin: Springer-Verlag, 2003.